Oligomeric amyloid β associates with postsynaptic densities and correlates with excitatory synapse loss near senile plaques

Robert M. Koffie[a], Melanie Meyer-Luehmann[a,b], Tadafumi Hashimoto[a], Kenneth W. Adams[a], Matthew L. Mielke[a], Monica Garcia-Alloza[a], Kristina D. Micheva[c], Stephen J. Smith[c], M. Leo Kim[d], Virginia M. Lee[d], Bradley T. Hyman[a], and Tara L. Spires-Jones[a,1]

[a]Neurology Department, Massachusetts General Hospital, Charlestown, MA 02129; [b]Department of Biochemistry, Laboratory for Neurodegenerative Disease Research, Ludwig-Maximilians-University, 80336 Munich, Germany; [c]Department of Molecular and Cellular Physiology, Stanford University School of Medicine, Stanford, CA 94305; and [d]Department of Pathology and Laboratory Medicine, University of Pennsylvania, Philadelphia, PA 19104

Edited by Floyd E. Bloom, The Scripps Research Institute, La Jolla, CA, and approved January 5, 2009 (received for review November 21, 2008)

Synapse loss correlates with a cognitive decline in Alzheimer's disease (AD), but whether this is caused by fibrillar deposits known as senile plaques or soluble oligomeric forms of amyloid β (Aβ) is controversial. By using array tomography, a technique that combines ultrathin sectioning of tissue with immunofluorescence, allowing precise quantification of small structures, such as synapses, we have tested the hypothesis that oligomeric Aβ surrounding plaques contributes to synapse loss in a mouse model of AD. We find that senile plaques are surrounded by a halo of oligomeric Aβ. Analysis of >14,000 synapses (represented by PSD95-stained excitatory synapses) shows that there is a 60% loss of excitatory synapses in the halo of oligomeric Aβ surrounding plaques and that the density increases to reach almost control levels in volumes further than 50 μm from a plaque in an approximately linear fashion (linear regression, $r^2 = 0.9$; $P < 0.0001$). Further, in transgenic cortex, microdeposits of oligomeric Aβ associate with a subset of excitatory synapses, which are significantly smaller than those not in contact with oligomeric Aβ. The proportion of excitatory synapses associated with Aβ correlates with decreasing density (correlation, −0.588; $P < 0.0001$). These data show that senile plaques are a potential reservoir of oligomeric Aβ, which colocalizes with the postsynaptic density and is associated with spine collapse, reconciling the apparently competing schools of thought of ''plaque'' vs. ''oligomeric Aβ'' as the synaptotoxic species in the brain of AD patients.

Alzheimer | array tomography | neurodegeneration | synaptotoxicity

Loss of connectivity caused by neuronal death and synapse loss is thought to underlie cognitive decline in neurodegenerative conditions, such as Alzheimer's disease (AD). Synapse loss appears to be particularly important in the pathogenesis of AD. Indeed, it is known that synapses are lost during AD and that in AD tissue, synapse loss correlates strongly with cognitive decline (1–3). There is a growing consensus, based primarily on cell-based assays, that amyloid β (Aβ), the main component of senile plaques, is toxic to synapses (4–6). In both AD patients and animal models of the disease, synapse loss is greatest near senile plaques, indicating a link between amyloid pathology and synaptotoxicity in vivo. Work by several groups has shown a decrease in dendritic spine density and synaptophysin-positive synapses radiating out from the surface of plaques in mouse models of AD (7–10). Whether this is caused by fibrillar plaques or soluble oligomeric Aβ is controversial. We used multiphoton imaging of the living brain to show that this spine loss is caused by impaired spine stability over time near plaques and postulated that a plaque-related diffusible bioactive molecule was responsible (11). Here, we test the hypothesis that oligomeric Aβ is directly synaptotoxic.

We hypothesize that soluble oligomeric Aβ associates with the postsynaptic density and causes the loss of synapses and spines observed around plaques. Previous studies into synapse density and molecular interactions at the synapse were limited by the small size of synapses, which approaches the limit of the z-resolution of conventional light, confocal, and multiphoton microscopy, causing conventional methods to overestimate synapse density and make it difficult, if not impossible, to detect subtle differences in synapse density and composition. We circumvent these problems by examining synapse density and the interaction of oligomeric Aβ with synaptic proteins with a new imaging technique called array tomography (12). Using this technique, we quantitatively assess plaque-associated excitatory synapse loss in a mouse model of amyloid deposition and demonstrate that a subset of postsynaptic densities interacts with microdeposits of oligomeric amyloid, particularly in a halo of oligomeric Aβ that surrounds the dense core of plaques. Density of postsynaptic densities (PSDs) decreases significantly near plaques in this model and correlates negatively with the proportion of oligomeric Aβ-positive PSDs. Importantly, PSDs that are associated with oligomeric Aβ are smaller than those in the same microenvironment that are not, implicating oligomeric Aβ in initiating an long-term depression (LTD)-like change in synaptic biology.

Results

Senile Plaques Contain, and Are Surrounded by, a Halo of Aβ Oligomers. We hypothesize that oligomeric Aβ surrounding senile plaques interacts with synapses and contributes to plaque-associated synapse loss. The first prediction of this hypothesis is that senile plaques contain or are surrounded by a halo of oligomeric Aβ. We tested this prediction by injecting AD transgenic mice (hereafter called APP/PS1 mice) that express mutant human presenilin 1 (DeltaE9) and a humanized mouse amyloid precursor protein with the Swedish mutation (13) with methoxy XO4 to label the dense core of plaques. We then topically applied the well-characterized, oligomer-specific NAB61 antibody (14) directly conjugated to a red fluorescent dye to the cortical surface and used multiphoton imaging to examine oligomeric Aβ in the living brain. Despite the low signal of the NAB61 antibody, oligomeric Aβ was clearly present in plaques and cerebral amyloid angiopathy (CAA), and there appeared to be a halo of oligomeric Aβ surrounding plaques in vivo (Fig. 1). To analyze the properties of this NAB61-positive halo quantitatively, we examined the relationship of NAB61 immunoreactivity to methoxy XO4 plaques in postmortem histological sections. We found that the dense cores of amyloid plaques indeed both contained and were surrounded by a halo of Aβ oligomers in this mouse model (Fig. 1). In 99 of 100 plaques

Author contributions: B.T.H. and T.L.S.-J. designed research; R.M.K., M.M.-L., T.H., K.W.A., M.L.M., and T.L.S.-J. performed research; K.D.M., S.J.S., M.L.K., and V.M.L. contributed new reagents/analytic tools; R.M.K., M.G.-A., and T.L.S.-J. analyzed data; and R.M.K., B.T.H., and T.L.S.-J. wrote the paper.

The authors declare no conflict of interest.

This article is a PNAS Direct Submission.

[1]To whom correspondence should be addressed. E-mail: tspires@partners.org.

This article contains supporting information online at www.pnas.org/cgi/content/full/0811698106/DCSupplemental.

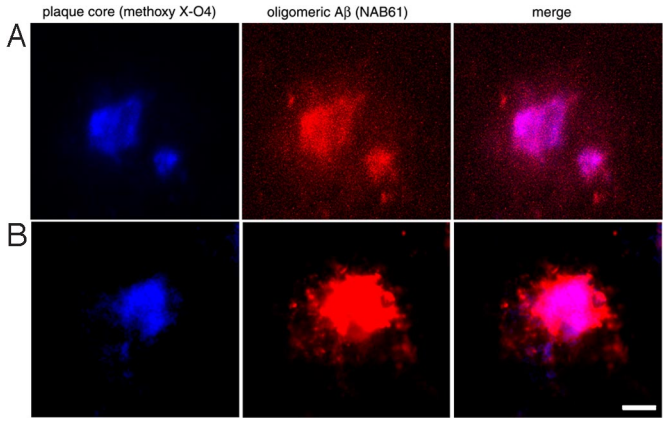

Fig. 1. Oligomeric Aβ is present in the dense core of amyloid plaques and in a halo surrounding the core. (*A*) NAB61 antibody conjugated to Alexa Fluor 594 (red) applied topically in vivo shows oligomeric Aβ surrounding dense plaques (labeled with methoxy XO4; blue). (*B*) Postmortem staining of dense plaques by using methoxy XO4 (blue) and oligomeric Aβ by using NAB61 antibody (red) confirms that oligomeric Aβ is found in the core of plaques and in an area surrounding the core. (Scale bar: 10 μm.)

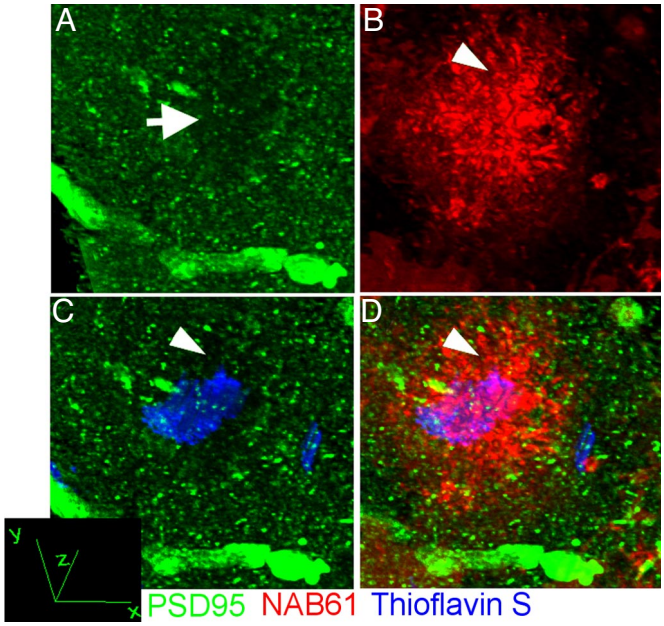

Fig. 2. A 3D reconstruction from array tomography images of a 60 μm × 60 μm × 20 μm volume of APP/PS1 cortex shows that a large volume of cortex around the dense core of the plaque (ThioS; blue) is occupied by a halo of oligomeric Aβ (NAB61 staining; red). Further, the 3D reconstruction illustrates that postsynaptic densities (PSD95 stain; green) are lost both within the plaque core (arrow; *A*), and in the area surrounding the core (arrowhead; *C*), which is within the halo of oligomeric Aβ (*B* and *D*).

analyzed, the area of NAB61 staining was larger than that of methoxy staining. On average, the NAB61-stained area was 556.7 ± 437.5 μm^2 larger than the methoxy staining, which only showed the dense core of the plaque [$P < 0.0001$, Student's t test; supporting information (SI) Fig. S1]. Assuming that plaques are approximately spherical, these data indicate that the halo of oligomeric Aβ surrounding each plaque core was 1.8 times the volume of the dense core, and the halo of oligomeric Aβ extended, on average, 6.5 ± 4.1 μm in all directions from the edge of the dense plaque. A 3D reconstruction of a plaque, core, halo, and surrounding synapses from an array tomogram illustrates the extent of the halo of oligomeric Aβ surrounding the plaque core (Fig. 2 and SI Movie S1).

Precise Quantification of PSD Loss near Amyloid Plaques. As seen in the reconstruction in Fig. 2, PSD staining was greatly reduced in the core of dense plaques and the area surrounding the core. It has been known for years that synapse loss occurs in AD and correlates with cognitive decline (1–3), and the association of amyloid plaques with local dendritic spine loss has been observed in mouse models of AD (7–9). Because we postulate that oligomeric Aβ acts at the PSD to cause spine loss, we have used array tomography to examine excitatory synaptic density specifically. We confirmed that the PSD95 antibody used is an accurate marker of PSDs in two ways: first by confirming colocalization with the NMDA NR2A subunit, and second by observing apposition of PSD95 puncta with synaptophysin-labeled presynaptic terminals (Fig. S2).

We examined excitatory PSDs in volumes at known distances from a plaque and in nontransgenic cortex to assess accurately the relationship between the presence of the plaque, of oligomeric Aβ, and PSD loss. A total of 3 APP/PS1 animals and 3 nontransgenic animals were used for analysis, with 8,890 synapses counted in 130 cortical sites in APP/PS1 cortex and 5,893 synapses counted in 67 cortical sites in nontransgenic cortex.

We found that compared with control animals, APP/PS1 transgenic mice had a 36.6% reduction in average excitatory synapse density, from 1.52E-9 ± 0.39E-9 PSD-labeled synapses per mm^3 in wild-type cortex to 9.64E-8 ± 4.63E-8 PSD-labeled synapses per mm^3 in APP/PS1 cortex (ANOVA $F_{1,195} = 71.148$, $P < 0.0001$). Excitatory synapse loss in APP/PS1 cortex was exacerbated near plaques, with significant decreases approaching the plaque edge (Fig. 3). Density of PSDs correlated with distance from halo edge (correlation coefficient, 0.706; $P < 0.0001$). In the dense core of the plaque, we found only rare PSD95-positive puncta (13 total puncta in 12 plaque cores analyzed of 8,890 total synapses counted in APP/PS1 mice), representing a 94% decrease from control synapse density (ANOVA genotype-independent variable split by distance from plaque, $F_{1,23} = 112.172$, $P < 0.0001$).

In the halo of oligomeric Aβ surrounding the plaque core, there was a 59% reduction in excitatory synapse density compared with control levels ($F_{1,23} = 39.737$, $P < 0.0001$). In volumes an average of 5 μm from the halo edge, there was a 40% decrease in PSD density compared with control levels ($F_{1,29} = 44.221$, $P < 0.0001$), and in volumes an average of 15 μm from the halo edge, there was a 28% loss compared with control levels ($F_{1,30} = 19.491$, $P = 0.001$). Synapse density increased in an approximately linear fashion from the edge of the plaque core to reach almost control levels in volumes further than 50 μm away from the nearest plaque (linear regression of average synapse density points excluding the plaque core, which is postulated to have no functional synapses; $r^2 = 0.901$, $P < 0.0001$). In nontransgenic cortex, distance to a randomly placed phantom plaque did not have any effect on synapse density ($P > 0.05$ in ANOVA and correlation tests).

As well as a decrease in excitatory synapse density in APP/PS1 cortex, we observed decreased PSD size. In wild-type cortex, PSD95 puncta had a median size of 0.033 μm^3, whereas in APP/PS1 transgenic cortex, PSD95 puncta were 0.019 μm^3, a reduction of ≈40% (Mann–Whitney test, $P < 0.0001$). This reduction in size did not change with respect to distance from the plaque (Kruskal–Wallis test, plaque distance as independent variable, split by genotype, $P > 0.3$ in both APP/PS1 and wild-type groups). Reduced spine size possibly indicates disrupted function in the remaining synapses, which are already fewer in number than control values, as seen above. A reduction in spine size could be functionally relevant because LTD is associated with dendritic spine shrinkage (15).

These data demonstrate, in a level of detail unattainable from standard immunohistochemical preparations, that excitatory syn-

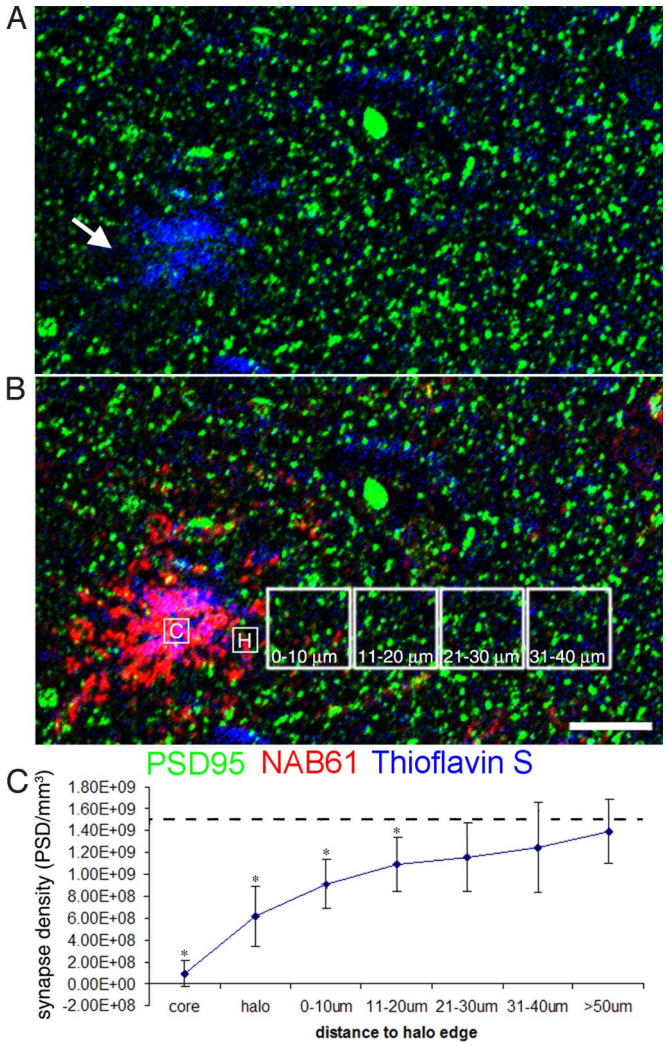

Fig. 3. Precise quantification of PSD loss using array tomography. Postsynaptic densities (PSD95; green), oligomeric Aβ (NAB61; red), plaque cores (ThioS; blue), and nuclei (DAPI; blue) were stained on ribbons of 70-nm sections of APP/PS1 and nontransgenic cortex (part of a single section from the APP/PS1 cortex shown in *A* and *B*). To quantify the relationship between synapse loss and proximity to a plaque, images were taken of the same area on serial sections, the volumes aligned, and PSD95 puncta density was analyzed. Volumes were chosen within the plaque core (box C in *B*), the halo of oligomeric Aβ surrounding the core (arrow in *A*, box H in *B*), and in volumes extending out from the edge of the halo in 10-μm increments. Quantification (*C*) reveals significant PSD loss compared with control cortex (dotted line shows control average, ANOVA PSD density-dependent variable, genotype-independent $F_{1,195} = 71.149$, $P < 0.0001$). Density of PSDs also decreases in APP/PS1 cortex in areas near plaques (ANOVA synapse density-dependent variable, distance category independent split by genotype $F_{6,123} = 36.323$, $P < 0.0001$; synapse density correlates with average distance from halo edge correlation coefficient 0.706, $P < 0.0001$). *, $P < 0.05$ ANOVA split by distance category comparison to control average. (Scale bar: 10 μm.)

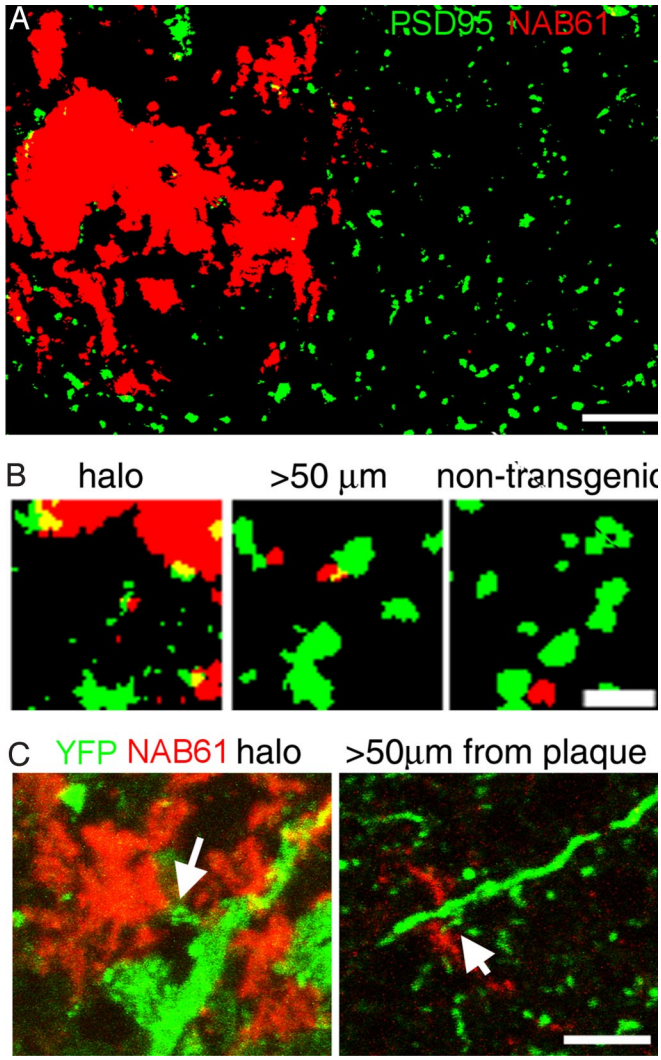

Fig. 4. Oligomeric Aβ associates with PSDs. (*A*) Projection of images of array sections (500-nm total thickness) that have been processed by using the watershed analysis program (thresholded and puncta present in only one section excluded) show postsynaptic densities (green) and oligomeric Aβ (NAB61; red). (*B*) Higher-resolution projections from within the halo of oligomeric Aβ surrounding a plaque further than 50 μm from a plaque in APP/PS1 transgenic mouse cortex and a volume from nontransgenic cortex show that oligomeric Aβ staining is present at some postsynaptic densities (yellow). (*C*) *Z*-projections of raw images from an array of a mouse transgenic for YFP (stained green in *C*) and APP/PS1 demonstrate that NAB61 puncta (red) contact dendritic spines (arrows point to spine heads, yellow shows colocalization) both in the halo of oligomeric Aβ surrounding a plaque and distant from plaques. (Scale bars: *A* and *C*, 5 μm; *B*, 1 μm.

apse density decreases progressively approaching plaques in a mouse model of plaque deposition.

Oligomeric Aβ Is Present at a Subset of PSDs and Correlates with Synapse Loss. Our observations suggest that there is a halo of oligomeric Aβ surrounding dense plaques in a region with ≈60% synapse loss and a linear increase in synapse density from the halo outward. We went on to test the hypothesis that oligomeric Aβ might be present at PSDs and account for the synapse loss radiating out from a plaque. We used array tomography to examine whether NAB61-positive microdeposits could be detected even outside the halo and, if so, whether NAB61 puncta were associated with synapses, and whether those synapses were specifically smaller than those not in contact with oligomeric Aβ.

We found that NAB61 labeled dense plaques, neuronal cell bodies, and small punctate microdeposits in the neuropil that were present both in the halo and extending out from the halo. Some PSDs were associated with microdeposits of oligomeric Aβ (Fig. 4). To confirm with an independent marker of postsynaptic sites that oligomeric Aβ contacts synapses, we stained arrays from an animal transgenic for both the APP/PS1 genes and yellow fluorescent protein (YFP) with NAB61. We confirmed that dendritic spine heads contacted NAB61-positive microdeposits of Aβ both within the halo of oligomeric Aβ around plaques and distant from plaques

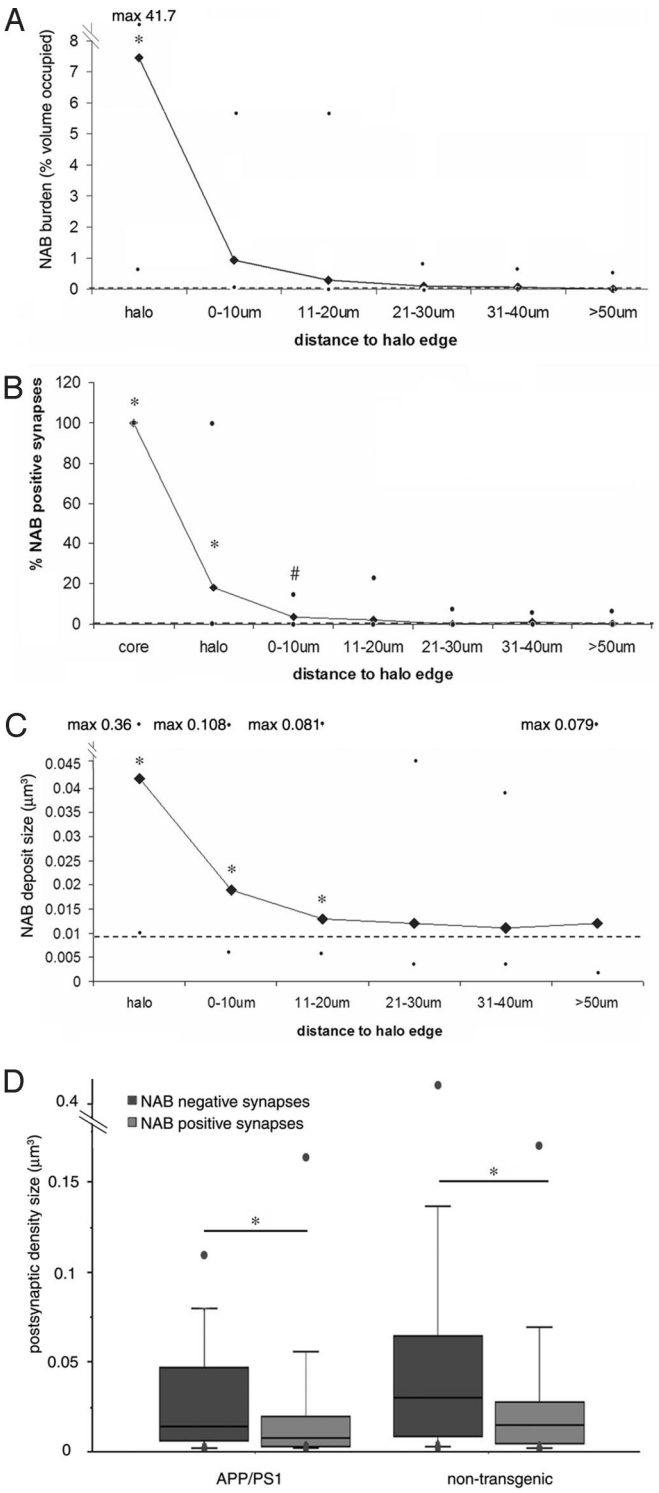

Fig. 5. Quantification of oligomeric Aβ deposits and their association with PSDs. (*A*) The burden of oligomeric Aβ (percentage neuropil volume occupied by NAB61 staining) is increased in the APP/PS1 cortex compared with wild type (dotted line) (Mann–Whitney test $P < 0.0001$). The oligomeric Aβ burden also increases in volumes closer to plaques in APP/PS1 mice (Kruskal–Wallis test, distance-independent variable, split by genotype APP/PS1, $P < 0.0001$). (*B*) The percentage of excitatory synapses positive for oligomeric Aβ staining increases near plaques in the APP/PS1 trasngenic cortex (Kruskal–Wallis test, $P < 0.0001$). Post hoc tests show that the percentage of PSDs interacting with oligomeric Aβ is significantly higher than nontransgenic levels in the plaque core and halo, and there is a trend toward an increase between 0 and 10 μm away from the edge of the halo. (*C*) NAB61 deposits are larger in APP/PS1 mice than in wild-type cortex (Mann–Whitney test $P < 0.0001$), with very large deposits occurring, particularly in the halo (maximum size, 0.36 μm^3). (*D*) A box plot of postsynaptic density size shows that PSDs are smaller in the APP/PS1 cortex than in nontransgenic cortex (Mann–Whitney test $P < 0.0001$), with a more substantial reduction in size in puncta associated with NAB61 deposits (Mann–Whitney test $P = 0.0026$). Even in nontransgenic brain, PSDs associated with oligomeric Aβ deposits are smaller than those not in contact with oligomeric Aβ (Mann–Whitney test $P = 0.0243$). Together, these data indicate that NAB61 interactions with the PSD may contribute to synapse loss. Data are not normally distributed and thus are presented as median with minima and maxima shown; control medians are dotted lines in *A*, *B*, and *C*. *, Post hoc Mann–Whitney tests $P < 0.05$; #, $P = 0.06$.

(Fig. 4). We further tested another antibody known to recognize oligomeric Aβ (R1282) and found that it associated with a subset of PSDs and costained puncta with NAB61, although the signal at the synapse was much weaker than that of NAB61 (Fig. S3). We also confirmed that NAB61 preferentially bound oligomeric species over monomers (14) in transgenic mouse brain lysates and cell culture preparations (Fig. S4).

The size of NAB61-positive oligomeric Aβ deposits outside of the dense core of plaques was variable, ranging from smaller than synapses (minimum, 0.002 μm^3), with the median value in transgenic cortex near the size of a synapse (0.01 μm^3), up to a maximum volume much larger than a synapse, resembling a "miniplaque" at 0.36 μm^3. In transgenic mice, these deposits were significantly larger than the 0.009-μm^3 median size in nontransgenic animals (Mann–Whitney test $P < 0.0001$), and there were deposits 10–40 times larger than the control median value in APP/PS1 cortex, particularly near plaques (Fig. 5). Because of the large variability in deposit size, instead of measuring density of oligomeric Aβ deposits, we measured neuropil volume occupied by NAB61 staining as a measure of cortical oligomeric Aβ burden (excluding plaque cores and cell bodies). This burden was higher in transgenic cortex than wild type (Mann–Whitney test $P < 0.0001$) and increased near plaques (Kruskal–Wallis test, distance-independent variable, split by genotype APP/PS1, $P < 0.0001$), coincident with the decrease in synapse density approaching the plaque.

In control cortex, 0.897% (median) of PSDs were positive for oligomeric Aβ staining (Fig. 5). In APP/PS1 cortex, the colocalization of PSD95 and oligomeric Aβ significantly increased near plaques, with 18% of synapses positive for oligomeric Aβ in the halo (Kruskal–Wallis test, distance-independent variable, split by genotype APP/PS1, $P < 0.0001$). We know that NAB burden is 7.5% in the halo and 1% in the 10-μm area immediately outside of the halo, and the volumes occupied by PSDs in these regions are 1% and 2%, respectively. Thus, there is only a 2 in 10,000 to 7 in 10,000 probability (0.02–0.07% chance) that these two stains would colocalize by chance. We observed 18% colocalization in the halo and 3.5% in volumes within 10 μm of the halo edge, >150 times chance levels, supporting the idea that microdeposits of oligomeric Aβ target the PSD. Although our hypothesis primarily concerns the effect of oligomeric Aβ at the PSD and its effect on spine loss, we also observed the expected loss of presynaptic material and occasional association of NAB61 staining with a marker of presynaptic vesicles (Fig. S5).

To examine the relationship between synapse density and the percentage of synapses that colocalize with oligomeric Aβ, we performed a statistical correlation of excitatory synapse density and percentage of NAB61-positive PSDs in the same volumes. This shows that density of PSDs negatively correlated with the proportion of synapses positive for oligomeric Aβ staining (correlation coefficient, −0.588; $P < 0.0001$). In further support of a synaptotoxic role of oligomeric Aβ, we observed that PSDs in contact with microdeposits of oligomeric Aβ were significantly smaller (median, 0.008 μm^3) than those not in contact with NAB61-positive puncta (median, 0.014 μm^3; Mann–Whitney test $P = 0.0026$). Proximity to

the plaque did not affect the size of spines contacting oligomeric Aβ deposits (Kruskal–Wallis test distance-independent variable, split by presence of NAB at the PSD, group with NAB61 staining, $P = 0.4733$), indicating that even far from plaques, oligomeric Aβ is harmful to synapses. In control animals, the small proportion of PSDs contacted by deposits of oligomeric Aβ also was smaller than those not contacted (medians, 0.015 μm^3 and 0.03 μm^3, respectively; Mann–Whitney test $P = 0.0243$), implying that oligomeric Aβ may play a physiological role in synaptic plasticity because smaller dendritic spines have been associated with LTD. Using Western blotting we confirmed that NAB61 recognizes nonmonomeric forms of Aβ in nontransgenic mouse brain and in lysates and conditioned media from the N2A mouse cell line (Fig. S4), indicating that the staining observed in nontransgenic brain is not artifactual.

These data show that oligomeric Aβ is present at the postsynaptic density in the brain, that it may play a role in synapse loss in AD, and further indicate a putative normal role for oligomeric Aβ in synaptic plasticity in the brain.

Discussion

Synapse loss is the strongest correlate of cognitive decline in AD (1), and senile plaques are associated with local synapse and dendritic spine loss (7, 8, 11). We postulated that bioactive plaque-associated molecules lead to spine instability and that some form of Aβ is involved because spine loss radiates outward from the surface of plaques, and anti-Aβ antibodies normalize this to some extent (16). Recent evidence strongly indicates that soluble forms of Aβ, including small Aβ oligomers, induce synaptic changes and dendritic spine loss in cultured neurons and organotypic slices (4, 5, 17–20), and an oligomeric form of Aβ correlates with memory loss in the Tg2576 mouse model (21, 22). However, these data do not discriminate between direct and indirect Aβ effects, or between fibrillar and oligomeric Aβ. Our current study uses two new techniques to examine these issues: first, array tomography allows detection of individual synaptic elements and their protein composition (12), providing the ability to directly examine the relationship of synapse loss to Aβ deposition; and second, we demonstrate the use of an oligomer-specific Aβ antibody to visualize specific conformational species of Aβ molecules (14).

We found that both postmortem and in vivo in a transgenic mouse model overexpressing mutant human amyloid precursor protein and presenilin, oligomeric Aβ can be detected within plaques and in a halo that surrounds the dense elements of the plaque and increases the volume by ≈180%. Using array tomography, we observed that density of PSDs decreased progressively approaching amyloid plaques in this model, ranging from almost normal density in volumes >50 μm from a plaque to almost complete loss of PSDs (94% decrease) in the dense core of plaques. Because of the space-occupying nature of the β-sheet structure of the plaque core, which is largely composed of Aβ, it is not surprising that there was almost complete loss of synapses in the core, and this correlates well with previous EM studies (23). We also observed a striking loss of PSDs (59.5% compared with control) in the area of cortex immediately surrounding the dense core, which was coincident with a halo of oligomeric Aβ surrounding the plaque. Finally, by using array tomography, we observed that oligomeric Aβ associated with a subset of PSDs in the APP/PS1 cortex, that this proportion increased in proximity to plaques, and that the PSDs contacted by microdeposits of oligomeric Aβ were reduced in size. We propose that the presence of oligomeric Aβ at the synapse may be toxic, contributing to plaque-associated synapse loss.

Based on these data, it is possible that oligomeric Aβ is within the synaptic compartments, as has been seen with EM (24), or that it is bound to the extracellular surface of the spine. Further analyses will be useful to determine the precise localization of oligomeric Aβ around or within synapses. Interaction of oligomeric Aβ with synapses may contribute to electrophysiological and behavioral deficits observed when it is injected into the brain (25, 26). Our results may also explain why transgenic mice treated with antibodies to remove oligomeric Aβ (NAB61, as used here) improve at spatial learning and memory tasks (14). Removing oligomeric Aβ from the synapse may prevent further synapse loss and allow synaptogenesis to occur or improve the function of synapses that had been associated with the microdeposits of oligomeric Aβ.

We observed shrinkage of PSDs in APP/PS1 transgenic mice, which was exacerbated in those synapses contacting microdeposits of oligomeric Aβ. These data imply that oligomeric Aβ affects PSD size. This could be associated with an LTD-like phenomenon because LTD has been associated with spine shrinkage (15), and in organotypic slice cultures, Aβ production has been shown to induce synaptic depression through the same pathways induced in LTD (6). In the APP/PS1 mice, shrinkage could result from interaction of oligomeric Aβ with the PSD, causing internalization of receptors, as seen in vitro (5, 6). PSD area is proportional to the number of postsynaptic receptors (27) and correlates with the number of presynaptic vesicles (28); thus, the size of the PSD is likely to be proportional to the reliability and strength of the synapse, indicating that shrinkage will affect synaptic activity. Our data show that oligomeric Aβ contacts PSDs directly in the brain and, together with these previous studies, support the hypothesis that oligomeric Aβ at the synapse impairs synaptic plasticity and leads to synapse collapse, thus contributing to synaptic dysfunction and cognitive impairment.

In summary, our data indicate that oligomeric Aβ may interact directly at the synapse to cause dysfunction and spine collapse. Together, the two observations that microdeposits of oligomeric Aβ surround plaques in a halo and extend into the neuropil, even far from plaques, and that the oligomeric Aβ is associated with a phenotype of PSD shrinkage and synapse loss, suggest a way to reconcile data that implicate either fibrillar Aβ or soluble oligomeric Aβ in neuronal dysfunction: that plaques act as a local reservoir of soluble oligomeric Aβ, which acts as a toxic moiety to synapses in the cortex.

Materials and Methods

Additional procedures are discussed in *SI Materials and Methods*.

Sample Preparation. To measure the size of the halo of oligomeric Aβ around plaques, AD transgenic mice (13) expressing mutant human presenilin 1 (DeltaE9) and a chimeric mouse/human amyloid precursor protein, APPSwe (called APP/PS1 mice, $n = 3$, age 9 months), were injected with methoxy XO4 (≈5 mg/kg i.p.) to label dense plaques. The next day, mice were killed with CO_2, and brains were extracted and fixed in 4% paraformaldehyde with 15% glycerol cryoprotectant. After postfixing at 4 °C for at least 48 h, brains were sectioned on a freezing microtome (Leica) at 50-μm thickness.

Sample preparation for array tomography was as outlined in ref. 12. Briefly, APP/PS1 mice ($n = 3$, ages 8–13 months) and nontransgenic controls ($n = 3$) were killed with CO_2. One animal expressing YFP and the APP/PS1 transgene (age 22 months) was also used for array tomography. Tissue samples (≈1 mm^3) were dissected from the somatosensory cortex and fixed in 4% paraformaldehyde, 2.5% sucrose in PBS for 3 h. The samples were dehydrated through ethanol and into LR White resin (Electron Microscopy Sciences) and polymerized overnight at 53 °C. Embedded blocks were cut into ribbons of 70-nm sections on an ultracut microtome (Leica) by using a Jumbo Histo Diamond Knife (Diatome).

Immunohistochemistry and Microscopy. For measurement of oligomeric Aβ around plaques, 50-μm floating sections were stained with an antibody specific to oligomers of Aβ (NAB61; ref. 14) and an anti-mouse Cy3-conjugated secondary antibody (Jackson ImmunoResearch). For array tomography analysis of excitatory PSDs and oligomeric Aβ, ribbons of 70-nm sections were rehydrated in 50 mM glycine in Tris-buffered saline and blocked in 0.05% Tween and 0.1% BSA in Tris. Primary antibodies [mouse anti-Aβ oligomers (NAB61) and goat anti-PSD95; Abcam] were applied at a 1:10 dilution in blocking buffer for 2 h, washed, and secondary antibodies (donkey anti-goat Alexa Fluor 488, Invitrogen; and donkey anti-mouse Cy3, Jackson ImmunoResearch) applied 1:50 in blocking buffer for 30 min. To stain plaques, 0.05% Thioflavin S in 50% ethanol was applied for 8 min before differentiation with 80% ethanol for 30 s. Sections were counterstained

with 0.01 mg/mL 4′-6-diamidino-2-phenylindole (DAPI) or mounted without nuclear stain.

For each area of interest (identified by fiduciary markers, such as plaques or nuclei), images were obtained on 7–20 serial sections through the somatosensory cortex. Images of 1,024 × 1,024 pixels were acquired by using a Zeiss Axioplan LSM510 confocal/multiphoton microscope (63× numerical aperture Plan Apochromatic water objective).

In Vivo Multiphoton Imaging. Transgenic animals (APP/PS1 transgenic, 8 months old) were anesthetized, and a cranial window was implanted as described (8, 29). Methoxy XO4 was injected (≈5 mg/kg i.p.) 1 day before window implantation. NAB61 directly labeled with Alexa Fluor 594 (kit from Molecular Probes) was applied topically to the brain after dura resection for 30 min before window sealing. Images of plaques in the living brain were acquired on a BioRad multiphoton microscope as described (8, 29).

Image Analysis and Statistics. Images were viewed and analyzed with Image J (National Institutes of Health open software). For analysis of oligomeric Aβ surrounding plaques, the blue channel (methoxy XO4) and red channel (NAB61) were opened separately, thresholded, and the edges of the stain outlined to determine the area occupied by the plaque core and oligomeric Aβ.

For array tomography data, each set of images was opened sequentially in Image J, converted to stacks, and aligned by using the MultiStckReg and StackReg plug-ins [courtesy of Brad Busse and P. Thevenaz *et al.* (30)]. Volumes at known distances from a plaque were selected, and an automated, threshold-based detection program was used to count puncta that appeared in more than one consecutive section (WaterShed program, provided by Brad Busse, Stephen Smith, and Kristina Micheva, Stanford University). An average PSD95-positive puncta density was calculated for each volume sampled. In APP/PS1 cortex, we sampled 130 sites in the cortex at known distances from a plaque (8,890 synapses total), and in nontransgenic cortex, we sampled 67 sites (5,893 synapses total) and assigned them distances from a phantom plaque for analyses.

Watershed exported a thresholded image stack (separate for each channel) showing puncta that were present in more than one slice of the array, and for each puncta it reported puncta size. In Image J, the output stacks from PSD95 and NAB61 staining for each region of interest were combined, and the number of PSD95 puncta with any pixels that colocalized with NAB61 were counted and the size of the PSD95 puncta contacting NAB61 deposits measured. A comparable number of randomly chosen PSD95 puncta without NAB61 staining were also measured for comparison, and these Image J measurements of 143 synapses were directly comparable with the automated measurements of thousands of synapses made by the WaterShed program. The percentage of NAB61-positive PSD95 puncta was calculated by dividing the number of NAB61-positive puncta by the total number of PSD95 puncta in each region of interest. Synapse densities were calculated by dividing the number of PSD95 puncta by the volume of tissue sampled.

Normality of data was assessed by using the Shapiro–Wilks test. Synapse density data, which were normally distributed, were analyzed by using ANOVA to compare mean synapse density of all volumes measured. Pearson correlations were used to determine correlations. Nonnormal data were compared by using Mann–Whitney *U* tests (for comparisons of 2 groups) and Kruskal–Wallis tests (for comparisons of >2 groups; for example, distances from a plaque edge). Calculated comparisons were at confidence interval 95%; i.e., $P < 0.05$ was considered significant. All values of normal data are reported in mean ± SD, and nonnormal data are presented as medians with minimum and maximum values.

ACKNOWLEDGMENTS. We thank Dr. Dennis Selkoe, Brigham and Women's Hospital, Boston for providing antibodies and Dr. Phill Jones, MGH, Boston for aid with image analysis. This work was supported by the Massachusetts Alzheimer's Disease Research Center National Institutes of Health (NIH) Grant 2 P50 AG05134-24, a John D. French Alzheimer's Foundation Fellowship, an Alzheimer's Drug Discovery Foundation grant, and NIH Grant AG08487.

1. Terry RD, *et al.* (1991) Physical basis of cognitive alterations in Alzheimer's disease: Synapse loss is the major correlate of cognitive impairment. *Ann Neurol* 30:572–580.
2. DeKosky ST, Scheff SW, Styren SD (1996) Structural correlates of cognition in dementia: Quantification and assessment of synapse change. *Neurodegeneration* 5:417–421.
3. Coleman PD, Yao PJ (2003) Synaptic slaughter in Alzheimer's disease. *Neurobiol Aging* 24:1023–1027.
4. Shankar GM, *et al.* (2008) Amyloid-β protein dimers isolated directly from Alzheimer's brains impair synaptic plasticity and memory. *Nat Med* 14:837–842.
5. Snyder EM, *et al.* (2005) Regulation of NMDA receptor trafficking by amyloid-β. *Nat Neurosci* 8:1051–1058.
6. Hsieh H, *et al.* (2006) AMPAR removal underlies Aβ-induced synaptic depression and dendritic spine loss. *Neuron* 52:831–843.
7. Tsai J, Grutzendler J, Duff K, Gan WB (2004) Fibrillar amyloid deposition leads to local synaptic abnormalities and breakage of neuronal branches. *Nat Neurosci* 7:1181–1183.
8. Spires TL, *et al.* (2005) Dendritic spine abnormalities in amyloid precursor protein transgenic mice demonstrated by gene transfer and intravital multiphoton microscopy. *J Neurosci* 25:7278–7287.
9. Knafo S, *et al.* (2008) Widespread changes in dendritic spines in a model of Alzheimer's disease. *Cereb Cortex*, in press.
10. Dong H, Martin MV, Chambers S, Csernansky JG (2007) Spatial relationship between synapse loss and β-amyloid deposition in Tg2576 mice. *J Comp Neurol* 500:311–321.
11. Spires-Jones TL, *et al.* (2007) Impaired spine stability underlies plaque-related spine loss in an Alzheimer's disease mouse model. *Am J Pathol* 171:1304–1311.
12. Micheva KD, Smith SJ (2007) Array tomography: A new tool for imaging the molecular architecture and ultrastructure of neural circuits. *Neuron* 55:25–36.
13. Jankowsky JL, *et al.* (2001) Co-expression of multiple transgenes in mouse CNS: A comparison of strategies. *Biomol Eng* 17:157–165.
14. Lee EB, *et al.* (2006) Targeting amyloid-β peptide (Aβ) oligomers by passive immunization with a conformation-selective monoclonal antibody improves learning and memory in Aβ precursor protein (APP) transgenic mice. *J Biol Chem* 281:4292–4299.
15. Zhou Q, Homma KJ, Poo MM (2004) Shrinkage of dendritic spines associated with long-term depression of hippocampal synapses. *Neuron* 44:749–757.
16. Spires-Jones TL, *et al.* (2009) Passive immunotherapy rapidly increases structural plasticity in a mouse model of Alzheimer disease. *Neurobiol Dis* 33:213–220.
17. Shankar GM, *et al.* (2007) Natural oligomers of the Alzheimer amyloid-β protein induce reversible synapse loss by modulating an NMDA-type glutamate receptor-dependent signaling pathway. *J Neurosci* 27:2866–2875.
18. Lacor PN, *et al.* (2007) Aβ oligomer-induced aberrations in synapse composition, shape, and density provide a molecular basis for loss of connectivity in Alzheimer's disease. *J Neurosci* 27:796–807.
19. Lambert MP, *et al.* (1998) Diffusible, nonfibrillar ligands derived from Aβ1–42 are potent central nervous system neurotoxins. *Proc Natl Acad Sci USA* 95:6448–6453.
20. Lacor PN, *et al.* (2004) Synaptic targeting by Alzheimer's-related amyloid β oligomers. *J Neurosci* 24:10191–10200.
21. Lesné S, *et al.* (2006) A specific amyloid-β protein assembly in the brain impairs memory. *Nature* 440:352–357.
22. Lesne S, Kotilinek L, Ashe KH (2008) Plaque-bearing mice with reduced levels of oligomeric amyloid-β assemblies have intact memory function. *Neuroscience* 151:745–749.
23. Lassmann H, Fischer P, Jellinger K (1993) Synaptic pathology of Alzheimer's disease. *Ann NY Acad Sci* 695:59–64.
24. Takahashi RH, *et al.* (2004) Oligomerization of Alzheimer's β-amyloid within processes and synapses of cultured neurons and brain. *J Neurosci* 24:3592–3599.
25. Walsh DM, *et al.* (2002) Naturally secreted oligomers of amyloid β protein potently inhibit hippocampal long-term potentiation in vivo. *Nature* 416:535–539.
26. Cleary JP, *et al.* (2005) Natural oligomers of the amyloid-β protein specifically disrupt cognitive function. *Nat Neurosci* 8:79–84.
27. Nusser Z, *et al.* (1998) Cell type and pathway dependence of synaptic AMPA receptor number and variability in the hippocampus. *Neuron* 21:545–559.
28. Harris KM, Stevens JK (1989) Dendritic spines of CA 1 pyramidal cells in the rat hippocampus: Serial electron microscopy with reference to their biophysical characteristics. *J Neurosci* 9:2982–2997.
29. Skoch J, Hickey GA, Kajdasz ST, Hyman BT, Bacskai BJ (2004) in *Amyloid Proteins: Methods and Protocols*, ed Sigurdsson EM (Humana, Totowa, NJ), pp 349–364.
30. Thevenaz P, Ruttimann UE, Unser M (1998) A pyramid approach to subpixel registration based on intensity. *IEEE Trans Image Process* 7:27–41.